

FAULT IDENTIFICATION IN AIR HANDLING UNITS USING PHYSICAL MODELS AND NEURAL NETWORKS

Ruxandra Dumitru and Dominique Marchio
Ecole des Mines de Paris
60, boulevard Saint-Michel
75272 Paris cedex 06

ABSTRACT

The main purpose of this paper is to *develop fault detection modules* for BEMS (Building Energy Management Systems), a software to aid building operators in detecting and diagnosing faults in HVAC systems. The fault detection modules proposed are based on two fundamentally different approaches based on component models: *physical models* and *neural net-works*. These modules using these two approaches are illustrated for a cooling coil of an Air Handling Unit. The parameters to be observed, the threshold (the limit over which the fault is considered), the sampling interval and the values of energy overconsumptions are established. The modules are then tested using data bases (no fault, fault) obtained from simulations of an HVAC system.

1. INTRODUCTION & BACKGROUND

A "fault" is defined as being a failure or unacceptable change in a property of a system or one of its components. One can distinguish three major types of faults: complete failure, malfunction and degradation.

To address these three types of faults standard fault identification (FD) methodology is built on two independent foundations: fault detection and fault diagnosis. In the first stage, the presence of the fault is detected and in the second the fault is located.

More specifically in the first stage, all the components with largest percentage of faults are identified. In [1], the analysis of causes of failures in different stages of an HVAC installation (design, assembling, commissioning, plant, equipment, operation, maintenance and training of the operators) was presented. The conclusion of [1] was that 29% of the faults result during the design stage, 21% in the maintenance stage, 12% in the assembling stage; all other stages provide faults in a proportion inferior or equal to 10%.

The classification of the components according to the number of faults is made by splitting up the HVAC system into sub-systems: ventilation, mixing section, air conditioning plant, cooling and heating plant, recuperation, air distribution, control system, safety installations and the sub-systems in components. For example, the air conditioning is

further split up into: cooling coil, heating coil and humidifier. The conclusion was that 33% of failures were caused by the heating and cooling plant, 14% by safety installations, 11% by ventilation and 10% by mixing section, all other systems being inferior to 10%. Carrying on this analysis down to the component level, the results are as follows: 8% of faults are provided by the humidifier, followed by fans and chiller with 7% and finally the water system with 5%.

With the above classification the next problem is the choice of a fault identification scheme. The criterion for a particular FD scheme in BEAMS should consider both robustness with respect to changes in the components and also generalize easily to other components and faults. In particular, the main issue is modeling the components. For example, in [12], fault identification using physical models supposes the description of the phenomena by heat and mass balance equations.

In an alternative approach, [3] ANN (*Artificial neural networks*) are used for components for which detailed models are not available or are not easy to explain from a physical point of view.

1.1 PROBLEM STATEMENT

In this paper, two fault detection modules based on physical models and a ANN are developed and compared for an Air Handling System.

Comparison between the two methods of fault detection is made for two components of the Air Handling Unit: the mixing section and the cooling coil. In this paper, the methodology is illustrated only for the cooling coil.

2. SYSTEM DESCRIPTION

The Air Handling System (single zone fan system) is illustrated in *Fig. 1*. In its most basic configuration, the Air Handling System provides constant volume, forced air heating and cooling for a single zone. (containing a heating coil, a cooling coil, filters (not shown), and a supply fan.) Normal operation assumes a mixed flow during the occupation period, between 7 a.m. and 8 p.m.

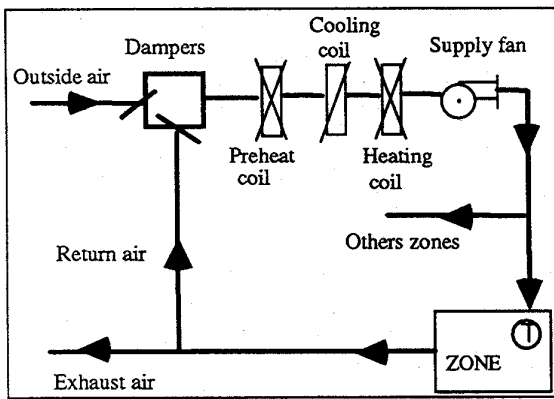


Figure 1. Schematic of Air Handling System.

It is further assumed that the quantity of outside air varies from "minimum required hygienic air", passing through "optimal mixing" to "all fresh air". The damper adjustment is driven by indoor temperature; its upper limit position is all-outside-air and its lower limit position is a mix of returned air with minimum required hygienic air.

The control of the cooling coil keeps the outlet temperature of the air constant for the same outdoor conditions.

3. FAULTS CONSIDERED

For the cooling coil, we considered two types of faults: **fouling on coil fins** and **scale in coil tubes**. The first fault leads to a reduction in overall heat transfer coefficient on the air side and the second fault to a reduction in overall heat transfer coefficient on the water side.

The cooling capacity decreases due to the fact that the heat transfer become gradually worse in both cases. As a result, the characteristic of the aerodynamic system changes, hence changing the operation point. The principal change is in the fan, in the case of 'fouling on coil fins' or the pump, in the case of 'scale in coil tubes', will operate at part load ratio. Hence, on the air side the fan's electrical consumption increases or, on the water side, the pump's electrical consumption increases as does the total energy consumption in one case or in another.

4. FAULT IDENTIFICATION

Both fault identification modules use the same measured values: the inlet air conditions (mass flow rate, temperature, and humidity ratio), the inlet water conditions (mass flow rate, temperature) and the outlet conditions of air and water. However some differences do exist. For example, the fault identification method using neural networks uses the cooling load, calculated on water side, therefore a combination of water parameters; meanwhile the fault identification method using physical models uses the water parameters one by one

(independently). Another is the fault identification scheme using physical models needs information about fan and pump energy consumption.

In the case of ANN, it is necessary to condition the data first [11]. The results of usual sensor measurements in a AHU, which includes flow rates, temperatures, humidity ratios, pressures, can vary significantly in magnitude and therefore must be appropriately conditioned. Consequently, normalized deviation values were used for the parameters. Calculation of the normalized deviation of a variable consists of taking the difference of the actual value and the average value of the variable, then dividing it by the average value. This data conditioning method produces the desired effect of scaling all the process variables within a similar range, maintaining the qualitative relationship between them.

5. FAULT IDENTIFICATION USING PHYSICAL MODELS

5.1. Description of the method

The *fault identification using physical models* relies on the comparison between the predicted values of different variables and the measured values of the same variables. The predicted values are the outputs of a physical model using measured values. The fault identification uses "if-then rules" and information concerning the other components called "complementary information" (energy overconsumption for example: see Section 5.4). This kind of information is needed during the diagnosis stage. When the deviation between predicted and measured values (temperature, humidity ratio) is larger than a certain threshold, the presence of a fault is declared. For the diagnosis, this kind of information is too the complementary information is then used.

5.2. Assumptions

The basic assumption is that the coil is operating under steady state conditions i.e. the coil dynamics are much faster than the other system components. Statistical methods [6], [5], [13], [14] based on statistics tests of mean, variance and slope [4], [7] were used in order to establish the time intervals when the coil is operating under steady state conditions.

The algorithm calculates the outlet water temperature, air dry bulb temperature and humidity ratio for a coil with a completely wet fin surface. The coil is considered to be operating under "all wet" surface conditions if the surface temperature at the air inlet is lower than the inlet air dew-point temperature. Under wet conditions, the steady state air and water conditions can be determined using

standard heat exchanger effectiveness relationships based on enthalpies rather than temperatures.

The resistances to enthalpy transfer are computed in terms of conventional heat transfer coefficients, fin efficiencies, and "fictitious enthalpy" parameters as described in Threlkeld [8].

5.3 Statistical method to determine steady-state

This statistical method implies three steps. First, each variable was considered separately with the null hypothesis that there was no difference in the variances from one period to the next. This was tested by the Fisher test on the ratio of the estimates of the variances from two successive periods. In cases where there was no significant difference between successive variances, the variances were pooled.

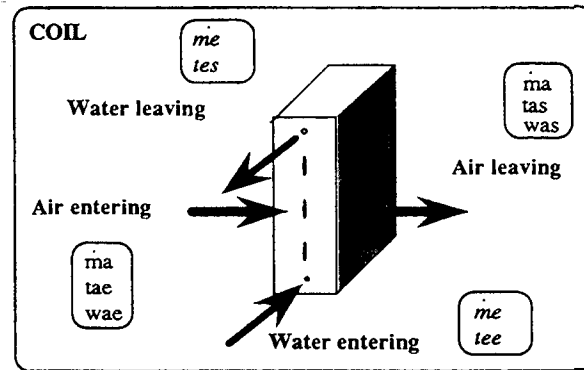
The Student test was then used to compare means of each measurement in successive periods, to find periods of apparent steady-state. Clearly it is sufficient in order to establish an unsteady-state to find a significant change in the mean of any measurement from one period to the next. To establish steady state, it is necessary but not sufficient to find a sequence of periods with no significant changes in the means of all measurements, since a trend could occur with small enough changes from one period to the next to escape statistical detection.

For each pair of time periods in succession, the means were tested against the null hypothesis that they are equal. If the null hypothesis could not be rejected, that pair was recorded as forming part of a sequence of periods in apparent steady state. As soon as a pair of means was found which had changed significantly-, if the earlier of the pair of periods already formed part of a sequence in apparent steady state, it marked the end of that sequence. Otherwise, the earlier period was flagged as unsteady state and in either case, the next pair of periods was examined. Any sequence of two or more successive time periods which remained unflagged were then considered to be in apparent steady state.

For each sequence of three or more periods of apparent steady state, we found the slope of the means of each measurement versus time from the first period to each later period. We then tested the null hypothesis that each slope was zero by a Student test. If any test failed, the sequence was shortened by excluding the subset of periods with significant slope. The sequence was either reduced to zero duration, or there remained a sub-sequence which was deemed to be in steady state. The slope test was intended to prevent slow monotonic trends and cyclic patterns from being taken as steady states.

5.4. Algorithm

The inputs and outputs for the coil model are schematically represented in Fig. 2.



Enthalpy based heat-transfer calculations for a wet surface use the fundamental relationship between heat transfer, enthalpy and capacity.

$$q_a = C_a \cdot (h_{ae} - h_{as})$$

$$q_e = C_e \cdot (h_{es,sat} - h_{ee,sat}) = \dot{m}_e c_e \cdot (t_{es} - t_{ee}) \quad (1)$$

where the capacity rate of the two fluid streams are:

$$C_a = \dot{m}_a \quad (2)$$

$$C_e = \dot{m}_e \cdot \frac{c_e}{c_{p,sat}} \quad (2)$$

$c_{p,sat}$ is calculate using the specific heat of dry air, the specific heat of water vapour and the humidity ratio of saturated air:

$$c_{p,sat} = c_a + w_{sat} \cdot c_v \quad (3)$$

The outlet air enthalpy and the enthalpy of saturated air at the water temperature can be determined by modeling the coil as a counterflow heat exchanger [12]. However, since the heat transfer calculations are performed based on enthalpies, the overall heat transfer coefficient is based on enthalpy potential rather than temperature potential. Under this assumption, a wet coil, local heat transfer and the corresponding overall heat transfer coefficient between the air and water are calculated by the following:

$$q = KS_h \cdot (h_a - h_{e,sat}) \quad (5)$$

The fault identification model compares the predicted values of the outlet variables, calculated with the algorithm that had been presented, with the measured values of the same variables. The measured values are noted with an apostrophy (') in the following identification scheme. Complementary information concerning the energy consumption (i.e. overconsumption of the circulation pump and overconsumption of the fan) is considered, as illustrated in Fig. 3.

circulation pump and overconsumption of the fan) is considered, as illustrated in Fig. 3.

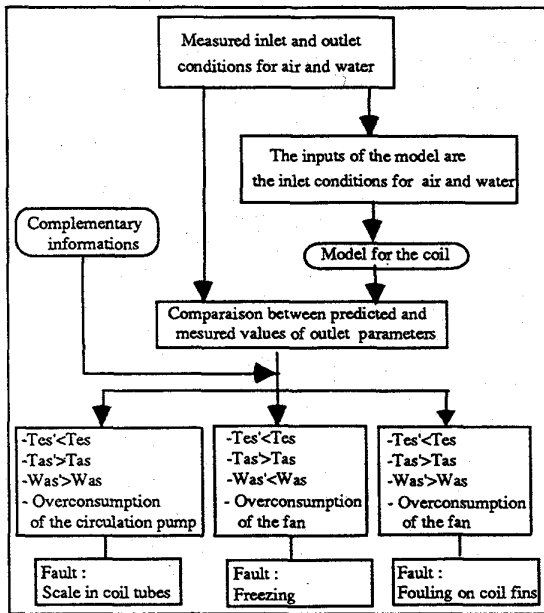


Figure 3. Fault identification model.

An example of one of the rules used in the above scheme is: the measured value of the air temperature exiting the coil, T_{as} is less than the expected value, T_{as}' (calculated with the algorithm). The explanation of this rule is that the considered faults (fouling, scaling or freezing) are sufficient to prevent the set-point being attained.

5.5. Application

This application of fault identification shows what kind of parameters are considered for fault detection. For example, outlet dry bulb temperature, the air's humidity ratio and cooling capacity were chosen to illustrate the consequences of each simulated fault. Hourly values of these parameters for a summer month (July), more precisely on 28th of July when the outside air temperature takes its maximal value 31°C at 4 p.m. are analyzed.

In the following examples, measurements for correct operation of the plant, called "reference values" (normal behavior), are compared to measurements for a non-optimal operation (failure). The last kind of operation is due to the appearance of the fault.

Both curves are obtained by simulation with DOE2. The DOE2 cooling coil model used is a bypass factor model.

The first simulated fault of the coil is the **scale in the tubes**. The effect of this fault is a decrease in the overall heat transfer coefficient between air and water, on the water side.

The reason is that scale in the tubes introduces a supplementary thermal resistance. The decrease in overall heat transfer coefficient leads to a decrease in heat transfer. Therefore on the water side the mass flow rate decreases resulting in less heat absorbed by the water. On the air side the mass flow rate remains constant but the difference of enthalpy decreases increasing the outlet air temperature and humidity ratio (Fig. 4).

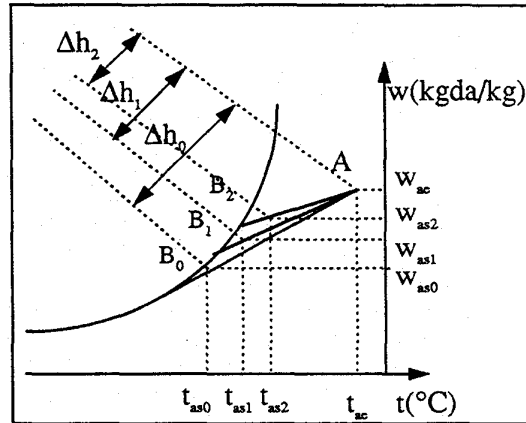


Figure 4: Influence of the overall heat transfer coefficient decrement.

In Fig. 4, the line AB_0 represents the cooling provided by the coil before scaling. In this case the difference of enthalpy is Δh_0 . After the introduction of scaling, the quantity of cooling becomes AB_1 with a corresponding difference of enthalpy Δh_1 . Consequently the outlet temperature and humidity ratio increase as does the surface temperature of the coil. Meanwhile as the scaling increases (line AB_2) the difference of enthalpy on air side, Δh_2 decreases which yields to a decreasing of the outlet air temperature and surface temperature of the coil.

The example in Fig. 5 shows the variation of the outlet air humidity ratio in this case. Note that, generally, the measurements of humidity may be reliable within about $\pm 3\%$ relative humidity for ordinary rooms temperatures under equilibrium conditions [8].

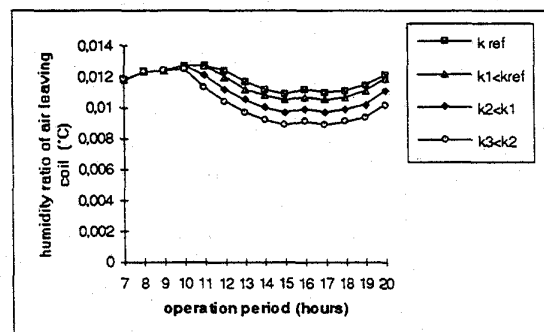


Figure 5. Scale in coil tubes - evolution of the humidity ratio of air leaving the coil.

The results concerning the observed parameters, thresholds, the sampling interval and values of energetic overconsumptions are given in *Table 1*.

The cooling capacity decreases and the energy consumption increases by 2% in the case of reduction in heat transfer coefficient of 6%, 5% for 16% reduction, 7% for 26%.

The second simulated fault is the **fouling on coil fins**. The heat transfer between air and water diminishes due to the decreasing of overall heat transfer coefficient on air side.

The parameters considered for illustrating the effect of the fault are: the outlet temperature and humidity ratio, the cooling coil capacity and the fan electrical consumption.

The hourly variations of the leaving air temperature is illustrated in the *Figure 6*.

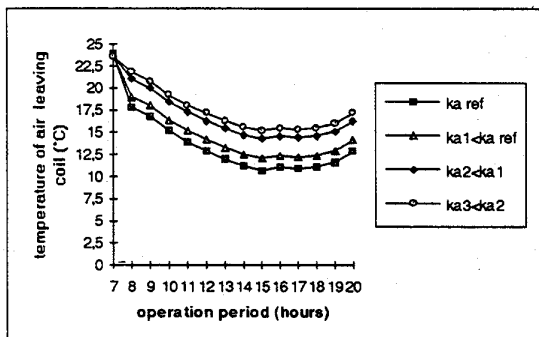


Figure 6. Fouling on coil fins - evolution of the air temperature leaving the coil.

A reduction in the overall heat transfer coefficient on air side of 20% (curve ka1) leads to a difference of temperature of 0.8°C between measured and reference values, which can not be detected. Meanwhile a reduction of 53% (curve ka2) of the overall heat transfer coefficient on air side determines a difference of temperature of 2.7°C, which is now measurable. A decrease of the overall heat transfer coefficient on air side of 66% induces a variation of temperature of 4°C (curve ka3). The temperature variation can be detected beginning by a reduction in the overall heat transfer coefficient on air side of 25%.

The fouling determines also a modification of aerodynamic characteristic of the system, the operation point changes and the fan operates at part load ratio leading to a waste of energy at the fan level.

The results concerning the observed parameters, thresholds, the sampling interval and values of energy overconsumption are also given in *Table 1*.

FAULT	Effect of the fault	Observed parameters ³⁾	Threshold ²⁾	Sampling interval	Energy consumption (in summer) ⁴⁾
scale in coil tubes ¹⁾	decrease of overall heat	6% humidity ratio of air	no	1 hour	-2%
		16% leaving cooling coil	yes	1 hour	+5%
		26% (kg/kg dry air)	yes	1 hour	+7%
	transfer coefficient on water side	6% coil surface	no	1 hour	
		16% temperature	yes C	1 hour	
		26% (°C)	yes C	1 hour	
fouling on coil fins ²⁾	decrease of overall heat	20% humidity ratio of air	no	1 hour	-2%
		53% leaving cooling coil	yes	1 hour	+5%
		66% (kg/kg dry air)	yes	1 hour	+10%
	transfer coefficient on air side	20% temperature of air	no	1 hour	
		53% leaving cooling coil	yes	1 hour	
		66% (°C)	yes	1 hour	
		cooling capacity (W)	yes	1 hour	

Table 1.

Obs: 1) The scale in coil tubes is a fault that can be detected starting by a diminution of 10% of the overall heat transfer coefficient on water side.

2) The fouling on coil fins is a fault that can be detected starting by a reduction of 25% of the overall heat transfer coefficient on air side.

3) Note that the number of observed parameters is larger than proposed in the identification scheme. Some of them can not be measured in practice. However, the fact that the data are provided by simulation allowed us to observe their evolution.

4) The values of the energy consumption are given only for the summer period. An augmentation of 10% in summer does not imply the same thing in winter.

5) It is considered that the temperature threshold is 1°C. Only the values superior to this threshold are taking into account for fault identification.

6. FAULT IDENTIFICATION USING ANN MODEL

6.1. Description of the method

The proposed fault identification methodology using ANN, supposes two stages [3], [9], [10].

First, the ANN learns the normal operation of the equipment. In this case, the ANN is trained and tested with data bases containing values of various parameters in the absence of fault. Note that this stage supposes two different operations: the learning and the testing of the network. Both are made with data bases representing the behavior without fault of the system, but not with the same. For example, in the coil case, the training is done with hourly values for the months of May and July and the testing with hourly values for the others months (August or September).

Second, the ANN is tested with an actual measured data base. The fault detection is based on the comparison between the outputs of the ANN for the normal operation with the outputs of the ANN for the actual measured data base. If the two sets of

outputs are different, we conclude that there is a fault.

After each test of the ANN, a representation of the predicted output versus real value is plotted. When the equipment is operating normally, the values from the testing data base are distributed in the proximity of the first bisectrix. When fault is present, the distribution of the testing data base values presents typical deviation from the first bisectrix (Fig. 7).

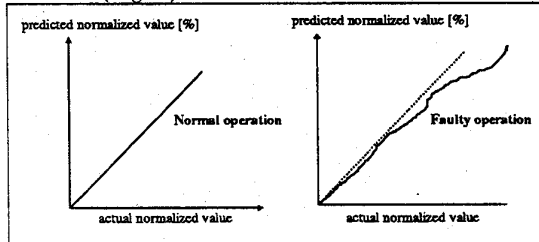


Figure 7. Representations of a predicted value versus a real value of an parameter.

6.2. Assumptions

The training of the ANN raises the problem of availability of data bases [9], [15]. In this approach, a minimum of 744 data pairs is needed for training. It is also important that these data corresponds to all possible situations of system operation. In the case of the cooling coil, the data used for training contain the hourly values of a month of mild weather. Suppose that only the month of August was chosen; in this case, the cooling coil operates in the most cases at maximum load. If the ANN is tested with the data bases for September, we note that the training was not efficient, because these data contains more operation situations than the training data.

6.3. Structure of the ANN

The ANN used for the fault detection in cooling coil has the following structure: 4 inputs, 3 outputs and 2 hidden layers containing 7, respectively 5 neurons (Figure 8). The inputs are the inlet air temperature, humidity ratio, mass flow rate and the cooling load. The outputs are the outlet air temperature and humidity ratio.

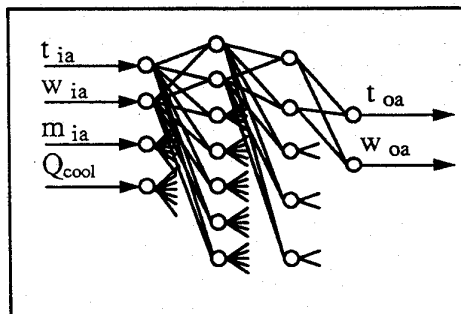


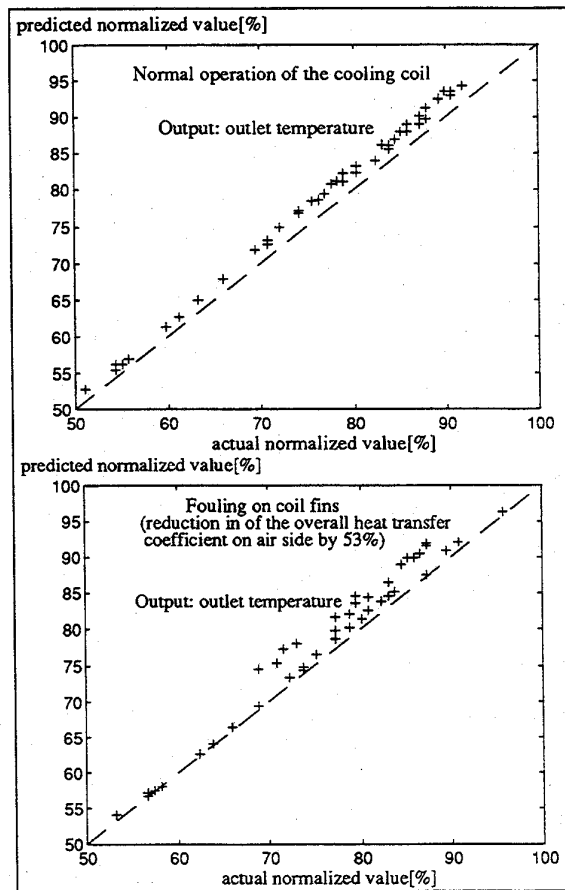
Figure 8. ANN for cooling coil.

Our generalized delta rule with backpropagation was used with a learning rate ϵ , of 0.9 and a momentum, μ of 0.1. A convergence criteria of 0.1, defined as the allowable difference between the actual output of a neuron in the output layer and the desired or target output, was used to determine the extent of further network training required.

6.4 Application

First, the ANN was trained under normal operation. For an efficient training, the data base must include the largest possible number of operating situations (the above mentioned months were chosen according to this purpose). The training data base contained hourly values for two months: May and July. The ANN was then tested using a data base for the month of August.

Next the ANN was tested using data bases representing faults: scale in coil tubes and fouling on coil fins, assuming various degrees of fouling and scaling. It may be seen that the deviation of the outputs with respect to the first bisectrix increases (Fig. 9).



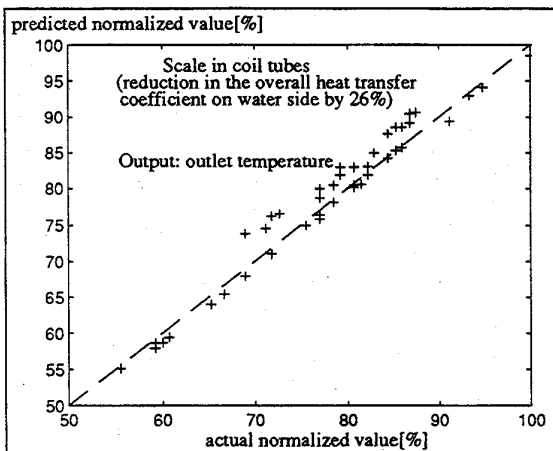


Figure 9. Increase of outputs deviation with respect to the first bisectrix due to the fault.

Fig. 9 is an example of the resulting graphical representations after the testing. The first graph represents distribution's of air temperature leaving the coil during the normal operation. In this graph the data base used for testing was the training data base. The distribution of the parameter is close to the first bisectrix (dashed line). The second graph represents the distribution of the same variable when fouling occurs determining a reduction in 53% of the overall heat transfer coefficient. Note that the distribution is no longer close to the bisectrix. The third graph represents the outlet air temperature distribution's when scaling occurs and a reduction in 26% of the overall heat transfer coefficient on water side is considered.

The relation between the evolution of the outlet parameters and the fault aggravation is given in the Table 2.

Faults	Outputs (outlet conditions)	air error (%)	RMS error (%)	Average error (%)	Maximum error (%)
Fouling on coil fins k air decrease of 20%	temperature (°C)	1.8	-1.0	-6.0	
	humidity ratio (g(dry air)/kg)	1.8	1.1	6.4	
Fouling on coil fins k air decrease of 53%	temperature (°C)	2.1	-1.3	-6.5	
	humidity ratio (g(dry air)/kg)	1.6	0.8	5.9	
Fouling on coil fins k air decrease of 66%	temperature (°C)	2.1	-1.3	-6.5	
	humidity ratio (g(dry air)/kg)	1.6	0.8	5.9	
Scale in coil tubes k water decrease of 6%	temperature (°C)	1.8	-1.0	-6.0	
	humidity ratio (g(dry air)/kg)	1.8	1.1	6.4	
Scale in coil tubes k water decrease of 16%	temperature (°C)	1.3	-0.5	6.3	
	humidity ratio (g(dry air)/kg)	1.5	0.9	5.4	
Scale in coil tubes k water decrease of 26%	temperature (°C)	1.5	-0.6	6.3	
	humidity ratio (g(dry air)/kg)	2.2	1.4	7.4	

Table 2.

CONCLUSIONS

One of the limits of using a physical model for fault identification in the coil case is that detailed information about the coil geometry is needed (heat transfer coefficient). For the neural networks data bases are needed.

Our results for fault identification with physical models, show that 'scale in coil tubes' fault can be detected with a reduction in 10% of the overall heat transfer coefficient on the water side and the 'fouling on coil fins' for a reduction in 25% of the overall heat transfer coefficient on the air side.

Values of the energy consumption are given for the summer period for different degree of fault (table 1) with the precaution that an augmentation of 10% in summer does not imply the same thing in winter.

A fault detection method based on neural networks has been developed.

The training time consists of 400 000 iterations in the coil case. The time is given in terms of iteration rather than specific durations, as actual physical training times are dependent on the speed of the computer used for training.

These two kinds of approaches have been tested using simulated data. The simulations are provided with DOE2 [2]. There are two kinds of data: data representing the normal operation of the system and data representing faulty operation of the system. The simulation of faults is introduced in DOE2 input files modifying the suitable parameters. Long term simulation data (yearly hourly values) and short running time are some of the advantages of choosing DOE2.

FUTURE WORK

A method of diagnosis using neural networks is under study. The training in this case uses data bases representing faulty operation of the system. A fault type is assigned to a particular output neuron which value is use to determine fault magnitudes.

If data base provided by simulation tools are used, the simulation period for a certain value of overall heat transfer coefficient had to be increased, because in fact the fouling on the coil and the scale in tubes are long-lasting phenomena. Until now, the simulated data were "non-continuous" because the data bases were created for different degrees of the fault. A future issue will be to take into account data describing the time evolution of the fault.

ACKNOWLEDGMENTS

The authors acknowledge ADEME (French Energy Agency) for supporting this work.

This research takes place also within a common international frame¹ of Annex 25 of IEA about fault identification in AHU systems.

REFERENCES

- [1] SCHIEL H.F., "Questionnaire modules of ventilation & air conditioning plants", Annex 25, - Building optimisation and fault detection, mars 1992 - Helsinki
- [2] DOE2, "Engineers Manual", Lawrence Berkely Laboratory, University of California, 1981
- [3] CURTISS S.P. "Artificial Neural Networks for use in building systems Control and Energy Management", thesis University of Colorado, 1992
- [4] CROWE C.M, HOLLY W., COOK R. (1989), "Reconciliation and rectification of process flow and inventory data", Canadian Journal of Chemical Engineering, vol.67, pp. 595-601, 1989
- [5] NEUILLY M., CETAMA, "Modélisation et estimation des erreurs de mesure", Lavoisier, 1993
- [6] RAGOT J., DAROUACH M., MAQUIN D., BLOCH G., "Validation de données et diagnostic", Editions Hermes, 1990
- [7] MEYER M., "Validation de données sur des systèmes incompletement observés", thèse de doctorat de l'Institut National Polytechnique de Toulouse, juillet 1990
- [8] THRELKELD J.L., "Thermal Environmental Engineering", 2nd Edition, Englewood Cliffs: Prentice Hall, 1970
- [9] HOSKINS J.C., HIMMELBLAU D.M., "Artificial Neural Networks Models of knowledge representation in chemical engineering", Computers & Chemical Engineering, volume 12, no.10 ,1988 p.881-890
- [10] KOSHIJIMA I., NIIDA K., "Neural Networks Approach to Fault Detection under steady state conditions", IFAC Symp. On - line Fault Detection and Supervision in the Chemical Process Industries, 1992, Newark,DE
- [11] BECRAFT W.R., LEE P.L., "An Integrated Neural Network/Expert system approach for fault diagnosis", Computers & Chemical Engineering, vol.17, no.10, pp. 1001-1014, 1993

- [12] HVAC2 Toolkit, Algorithms and Subroutines for Secondary HVAC System Energy Calculations, ASHRAE, 1791 Tullie Circle N.E., Atlanta, 1993
- [13] SAGE A. P., MELSA J.L., "Estimation Theory with Application to Communications and Control", New York:McGraw Hill, 1970
- [14] VAN TRESS H.L., "Detection, Estimation and Modulation Theory", Part I and Part III, New York:John Wiley & Sons, 1971
- [15] Yan H. H., Fischl R. and Chow J. C., "Indices for evaluation of neural network performance in power system security assessment," ISAP, Montpellier, France, Sept. 5-9, 1994.

NOMECLATURE

- C_a = air-side capacity rate	(kg/s)
- C_e = water-side capacity rate	(kg/s)
- h_{ae} = entering air enthalpy	(J/kg)
- h_{as} = leaving air enthalpy	(J/kg)
- \dot{m}_e = entering water mass flow rate	(kg/s)
- \dot{m}_a = dry air mass flow rate	(kg(da)/s)
- t_{ae} = entering dry bulb temperature	(°C)
- t_{as} = leaving air temperature	(°C)
- w_{ae} = entering air humidity ratio	(kg/kg da)
- w_{as} = leaving air humidity ratio	(kg/kg as)
- t_{ee} = entering water temperature	(°C)
- t_{es} = leaving water temperature	(°C)
- c_a = specific heat of air = 1006	(J/kg°C)
- c_v = specific heat of water vapor = 1830	(J/kg°C)
- c_e = specific heat of water = 4186	(J/kg°C)
- KS_h = overall enthalpy heat transfer coefficient	(kg/s)
- " e_{sat} " = "fictitious enthalpy" (enthalpy of saturated air evaluated at the liquid chilled water temperature)	

¹ Annex 25 "Real simulations of HVAC Systems for building optimisation, fault detection and diagnosis" is a part of the programme "Energy Conservation in Buildings and Community Systems" of the IEA, International Energy Agency.